CrossMark

ORIGINAL PAPER

Engineering cellulose nanofibre suspensions to control filtration resistance and sheet permeability

Qing Li · Praveena Raj · Fatema Abbas Husain · Swambabu Varanasi · Tom Rainey · Gil Garnier · Warren Batchelor

Abstract This study examines and quantifies the effect of adding polyelectrolytes to cellulose nanofibre suspensions on the gel point of cellulose nanofibre suspensions, which is the lowest solids concentration at which the suspension forms a continuous network. The lower the gel point, the faster the drainage time to produce a sheet and the higher the porosity of the final sheet formed. Two new techniques were designed to measure the dynamic compressibility and the drainability of nanocellulose–polyelectrolyte suspensions. We developed a master curve which showed that the independent variable controlling the behaviour of nanocellulose suspensions and its composite is the structure of the flocculated suspension which is best quantified as the gel point. This was independent of the type of polyelectrolyte used. At an addition level of 2 mg/g of nanofibre, a reduction in gel point over 50 % was achieved using either a high molecular weight (13 MDa) linear cationic polyacrylamide (CPAM, 40 % charge), a dendrimer polyethylenimine of high molecular weight of 750,000 Da (HPEI) or even a low molecular weight of 2000 Da (LPEI). There was no significant difference in the minimum gel point achieved, despite the difference in polyelectrolyte morphology and molecular weight. In this paper, we show that the gel point controls the flow through the fibre suspension, even when comparing fibre suspensions with solids content above the gel point. A lower gel point makes it easier for water to drain through the fibre network, reducing the pressure required to achieve a given dewatering rate and reducing the filtering time required to form a wet laid sheet. We further show that the lower gel point partially controls the structure of the wet laid sheet after it is dried. Halving the gel point increased the air permeability of the dry sheet by 37, 46 and 25 %, when using CPAM, HPEI and LPEI, respectively. The resistance to liquid flow was reduced by 74 and 90 %, when using CPAM and LPEI. Analysing the paper formed shows that sheet forming process and final sheet properties can be engineered and controlled by adding polyelectrolytes to the nanofibre suspension.

Keywords Cellulose nanofibre · Gel point · CPAM · PEI · Dewatering · Permeability · Polyelectrolyte

Qing Li and Praveena Raj have contributed equally to this work.

Q. Li · P. Raj · F. A. Husain · S. Varanasi · G. Garnier · W. Batchelor (✉)
BioResource Processing Research Institute of Australia (BioPRIA), Department of Chemical Engineering, Monash University, Clayton, VIC 3800, Australia
e-mail: warren.batchelor@monash.edu

T. Rainey
School of Chemistry, Physics and Mechanical Engineering, Queensland University of Technology, Brisbane, QLD 4000, Australia

🍀 Springer

Introduction

Cellulose, the most abundant biopolymer on our planet, is present everywhere and every day brings new applications and industrial use. Cellulose is a polysaccharide, primarily produced by plants via photosynthesis. Existing as a reinforcing structure in most plants, it is not only easy to produce and access, but also environmentally friendly. Turbak et al. (1983) first obtained cellulose microfibrils by extracting them from wood cells using a mechanical disintegration process. A "microfibril" generally describes a fibrous cellulose structure that is 2–100 nm thick and length generally in the micron range (Siró and Plackett 2010). Both "nanofibril" and "nanofibre" have been used interchangeably with "microfibril". Micro-fibrillated cellulose (MFC) shows a web like structure (Lu et al. 2008) with fibrils and greatly expanded in surface area (Nakagaito and Yano 2005). Cellulose nanofibres have many advantages in comparison to conventional pulp fibres. Firstly, cellulose nanofibres have superior mechanical, thermal and barrier properties (Syverud and Stenius 2009); secondly, its biodegradability and renewability compared to other artificial nanofibres; and low cost makes it economically attractive (Syverud and Stenius 2009). MFC nanofibres has potential for high stiffness since the Young's modulus of the cellulose crystal reaches 134 GPa (Sakurada et al. 1962). High stiffness and low density makes cellulose nanofibre a natural reinforcing material. Cellulose nanofibres can form a complete fibrous network with very small size pores when formed as sheet, which is difficult for gas to permeate through (Fukuzumi et al. 2008). Due to these superior properties, cellulose nanofibre is a promising material for filters and barriers.

Filtration and casting are the two most common methods used for preparing nanofibre sheet. However, both methods are time consuming (Sehaqui et al. 2010). Evaporation of water during casting takes more than 48 h. During filtration, nanofibre suspension does not drain fast (Sehaqui et al. 2010). Decreasing the nanofibre sheet preparation with low energy cost remains a challenge (Zhu et al. 2014). Sheet forming properties such as drainage time and retention of nanofibres and sheet properties have been shown to be directly related to the suspension gel point (Raj et al. 2015; Varanasi and Batchelor 2014).

In the past, water soluble polymers have been added to cellulose nanofibres suspension to alter the rheological properties of the suspensions (Lowys et al. 2000; Nanko and Pan 2003; Vesterinen and Seppala 2008; Mosse et al. 2012), to improve the nanofibre sheet forming characteristics and the mechanical properties of nanofibre sheet (Varanasi and Batchelor 2014). Addition of cationic polymers has also been shown to significantly reduce the suspension gel point (Raj et al. 2015). Gel point is defined as the lowest fibrous volume fraction at which all the primary flocs are interconnected and form a self-supporting network (Nasser and James 2006; Landman et al. 1988; Varanasi et al. 2013). Above the gel point, the suspension has compressive yield stress. Compressive yield stress is defined as the value of network pressure at which a flocculated suspension at a particular volume fraction will no longer resist compression and start to yield. This is the stress which must be exceeded by an applied load before network consolidation can occur which increases the fiber local volume fraction (Nasser and James 2007). The compressive yield stress is strongly affected by the strength of the inter-particle bridging forces and will determine the resultant floc sizes and internal structure. Stronger flocs have a higher resistance to consolidation and hence, higher compressive yield stresses.

Recently, we found that addition of either a cationic polyacrylamide (CPAM) or a Polyamide-amine-epichlorohydrin (PAE) to MFC suspension at an addition level of 2 mg/g of MFC and 10 mg/g of MFC, respectively, reduced the MFC suspension gel point from 1.7 to 0.5 and 1 kg/m^3, respectively (Varanasi and Batchelor 2014). A suspension with a lower gel point has a higher sediment volume, i.e. the sedimented layer at a given solids content will be thicker. Hence the sediment volume of MFC and CPAM or PAE suspensions is higher than for the MFC suspension alone. Increasing the sediment volume increases the dewatering rates because a bulky and porous mat is formed (Hubbe et al. 2007). Recently we reported that the drainage time of a cellulose nanofibre suspension into a film was reduced by 2/3 by reducing the gel point from 0.2 to 0.1 kg/m^3, by adding CPAM; this was due to the more flocculated suspension facilitating drainage (Raj et al. 2015). Hence, drainage rate of MFC suspension decreased with the addition of either CPAM or PAE while increasing the porosity of

the sheet signifying that a more open structure of the cellulose nanofibres is obtained after drying (Varanasi and Batchelor 2014; Raj et al. 2015).

Although we have found that a cationic polymer does play a role in reducing the sheet formation time, many questions arise. These include: (1) how does gel point relate to porosity, permeability and sheet forming for different polymers at a range of dosages? (2) Can we accurately control porosity? (3) What effect does polymer morphology have? (4) What are the optimum levels of polymer addition for different types of polymers?

In this paper, we extended our previous studies in two significant ways. Firstly we investigated polyethylenimine (PEI), a polyelectrolyte dendrimer widely used for surface modification. The PEI morphology upon adsorption and its coagulation mechanism differ from those achieved with high molecular weight CPAM. Secondly, we investigated the effect the type of polymer has on the quality of nanocellulose fibre suspension and the properties of the resulting sheet, especially permeability to gas and liquid flow. The porosity and pore size of nanofibre networks are important elements in filtration and barrier applications. It is the objective of this study to analyse to which extent the coagulating type of polyelectrolyte can be used to engineer fibrous network and pore size to improve cellulose nanofibre sheet performance as filters and barriers.

Experimental methods

Materials

Micro fibrillated cellulose (MFC) purchased from Daicel Chemical Industries Limited (grade Celish KY-100S) with 75 % moisture content was used. The cationic polyacrylamide (CPAM) polymer was kindly supplied by AQUA + TECH Switzerland from their SnowFlake Cationics product range, and used as received. The CPAM used is a copolymer of uncharged acrylamide with cationic dimethylaminoethylacrylate methyl chloride and has a measured charge density of 1.02×10^{-3} eq/g (40 % as reported by manufacturer) and a molecular weight of 13 MDa. Polyethyleneimine (PEI) solution of molecular weight of 750 and 2 kDa (50 wt% in H_2O) were purchased from Sigma Aldrich. These samples are denoted as HPEI and LPEI, respectively. Using titration method, the charge

density of HPEI and LPEI were found to be 1.93×10^{-3} and 3.37×10^{-4} eq/g, respectively. Ultrapure water purified with a Millipore system (18 MΩ cm) was used in all aqueous solutions and rinsing procedures.

Nanofibre-polyelectrolyte suspension preparation

A disintegrator equipped with a small propeller and a 3 L vessel was used to disperse nanofibres in water evenly by running the propeller for 15,000 revolutions. CPAM solutions were prepared by mixing the calculated amount of distilled water with the exact amount of CPAM powder in a beaker, to make a 0.5 mg/mL solution, using a magnetic stirrer. A minimum of 8 h was allowed for the mixing process. PEI solutions were diluted from the 50 wt% solution to 0.5 mg/mL solution and stirred for a minimum of 2 h before use. Fresh samples of CPAM and PEI solution were prepared daily.

Gel point measurement

The gel point is the lowest solids concentration where the fibres can form a continuous network in the suspension. In the past, gel points for wood fibres have been obtained through a sedimentation method which was first introduced by Martinez et al. (2001). The method has been adapted to nanocellulose suspensions by Zhang et al. (2012) and subsequently shown to correlate well to yield stress measurements of gel point (Varanasi et al. 2013). The measurement and analysis method used in this study to obtain the gel point of nanofibre suspensions is improved from the earlier studies and is similar to that described in Raj et al. (2015).

To measure the gel point, 250 mL of nanocellulose suspension with solids concentration (= solids fraction × suspension density) ranging from 0.05 to 0.025 wt% were prepared. The suspension was agitated using a hand stirrer to ensure even distribution of the nanofibres before polymer solution was added at the required addition level, to form the nanocellulose–polymer suspension. The composite suspension was then agitated using a hand stirrer for 2 min to suspend the fibres completely and allow for floc formation. Once the nanocellulose composite suspension had settled down completely, the height of sediment in the cylinder was measured. A minimum of 48 h was

allowed to ensure equilibrium for the sedimentation process. This procedure was repeated at different initial suspension concentrations and the ratio of sediment height (h_s) to initial height (h_0) was recorded as a function of initial solid concentration (C_o). The initial height was held constant from test to test and set at 23.7 cm. A graph of initial solid concentration (C_o) versus the ratio of sediment height (h_s) to initial suspension height (h_o) was plotted using the Curve Fitting Tool in Matlab (Raj et al. 2015). A smoothing spline was fitted to the data with smoothing parameter of 0.9996. The first derivative of each curve was also plotted. The constant y-intercept value at the origin of the first derivative curve then gives the gel point.

Nanofibre suspension dewatering force measurement

The test was carried out in a compression load cell similar to the method described in (Rainey et al. 2011). The load cell is made up of a barrel mounted on a base and a platen which is connected to an Instron Model 5566. The platen with diameter 81 mm contains 30 holes of ID 6 mm, for a total area of 8.48 cm^2, to allow water to flow through the platen when compressing the MFC suspension. A filter mesh wire with pore size of 125 μm, is attached to the bottom of the platen to prevent any nanofibres from leaking through the mesh and an O-ring is installed around the platen to prevent leakage from the sides. For each dewatering experiment, a new batch of 200 mL of either 0.15 wt% MFC suspension alone or with the selected amount of CPAM polymer was used. The addition levels studied ranged from 1 to 10 mg CPAM/g of MFC. The suspension was mixed with the CPAM for 2 min to ensure good distribution prior to adding it to the barrel.

The experiment was started with the platen 50 mm above the base. Filtration was carried out by lowering the platen at a rate of 3 mm/min until it was 10 mm from the base. The plot of the compression load versus the compression distance generated by the Instron was used for calculating maximum load of dewatering, hence, the dewatering pressure. The maximum load that was obtained at a platen displacement of 37 mm was used as the dewatering force. Each experiment was repeated three times. Three replicates for MFC and MFC + CPAM suspension are shown in Fig. 1, which reveals the reproducibility of experiments. It is interesting to note that the maximum load decreased

after 37 mm when CPAM was added to MFC suspension. This maximum might be related to the structure of the critical floc defined by the type of nanocellulose. We speculate that the decrease in load after 37 mm extension could be due to the change of structure and realignment of the fibres in suspension at high solids content, forming channels for better flow. This could result in a reduction in the compression load needed to drive the platen through the suspension. This should be part of a further study to investigate the load at different extensions of MFC-polymer suspensions.

Nanofibre membrane formation

Standard eucalyptus handsheets were constructed as support for a membrane layer of MFC. 60 g/m^2 NIST hardwood sheets were prepared according to the Australian/New Zealand Standard Method 203s. The dry hardwood pulp was soaked overnight in water. The soaked pulp was then transferred to a disintegrator (Model MKIIIC, Messmer Instruments Ltd) and disintegrated for 75,000 revolutions. Hardwood sheets were made from a suspension of 0.1 wt% solid content. The thickness and apparent density of hardwood sheets were measured according to Australian/New Zealand Standard Methods 426s and 208s.

A 400 mL 0.075 wt% MFC suspension mixed with the required amount of polyelectrolyte for 2 min using a hand stirrer. The prepared hardwood sheet was placed on top of the mesh in an Automatic British Handsheet Maker and wetted. The mixed MFC and polyelectrolyte suspension was then gently poured into the handsheet maker, to form a 15 g/m^2 layer on hardwood sheet, forming the two layer membrane.

Nanofibre membrane properties

Air Permeability of the dry nanofibre membrane was measured using an L&W Permeance tester.

Water flow through the membrane was measured using the same instrument as for the dewatering experiment. Firstly, the 150 mesh size steel mesh was stuck to the bottom of the platen as a support, followed by the membrane. The sides were sealed. The load cell was filled up to 90 % of the maximum height with deionised water. The platen was then lowered until it was completely submerged. Filtration of water was
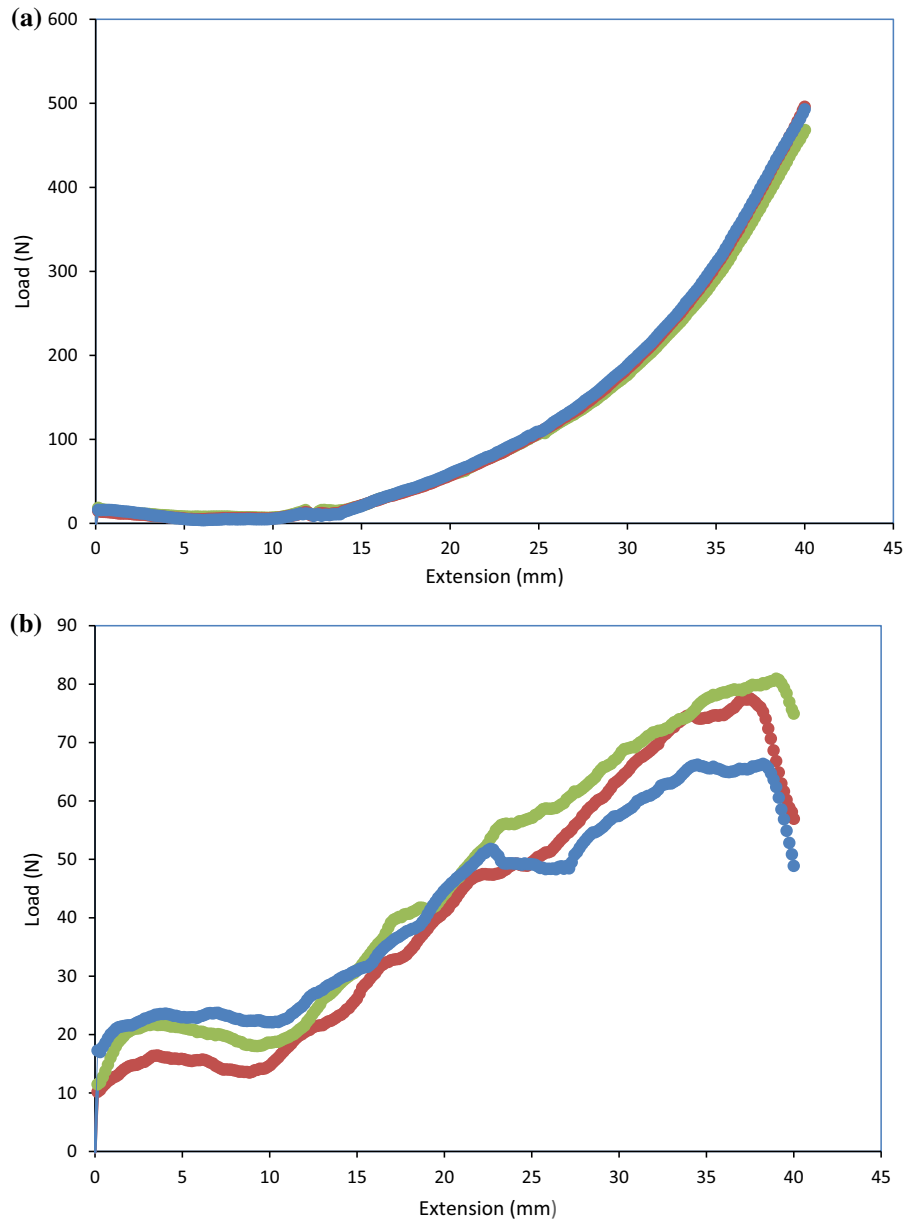
Fig. 1 Dewatering curves of MFC suspension: **a** without polymer, **b** with addition of 1 mg of CPAM/g of MFC. Three replicates are compared

carried out under constant compression rate of 0.1 mm/min (corresponds to flux of 36.5 LMH) until displacement reached 3 mm, after which the compression rate was increased to 0.2 mm/min (corresponds to flux of 72.9 LMH). A typical set of load versus extension data measured by Instron is shown in Fig. 2, which shows 3 measurement replicates for the MFC suspension mixed with CPAM at an addition

level of 1 mg/g of MFC. Dividing the plateau value of load at a given extension rate by platen open area gives the pressure at which water comes through the membrane at the cross-head speed.

Due to the much smaller pore size of the cellulose nanofibre layer compared to the conventional cellulose layer, the filtration properties are almost entirely determined by the nanofibre layer.

Fig. 2 Water flux measurements of a MFC–CPAM composite membrane at two different speeds of 0.1 mm/min (data up to 3 mm extension) and 0.2 mm/min (data above 3 mm extension) with a CPAM addition level 1 mg/g used in making the membrane. Three replicates are shown
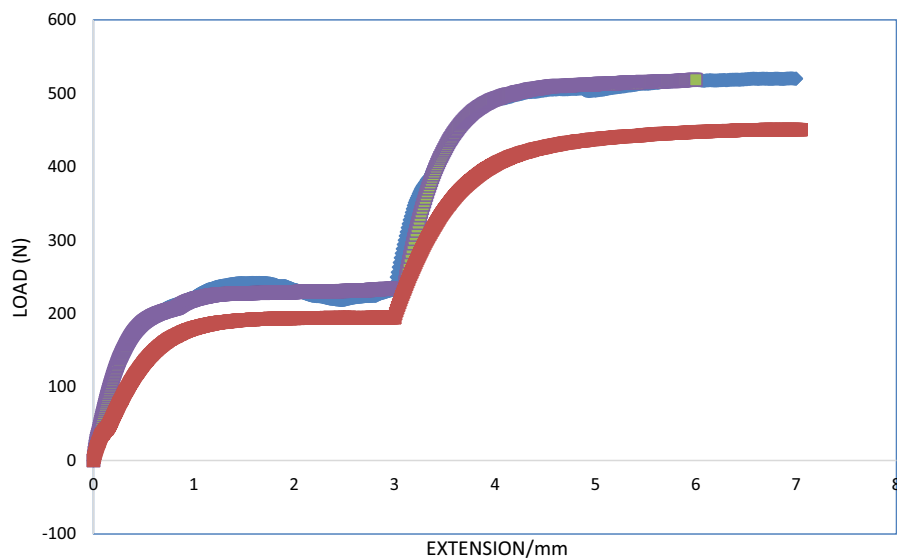
Results

Colloidal suspension measurements

Figure 3 shows that the polyelectrolyte addition significantly affects the gel point of cellulose nanofibre suspension. CPAM and PEI show two different types of influence on the MFC suspension. However, the gel point of CPAM at every point was higher than that of PEI. All lines show the same decreasing trend when small amounts of polymer were added. The gel point declined from 0.24 to 0.18 wt% for CPAM when
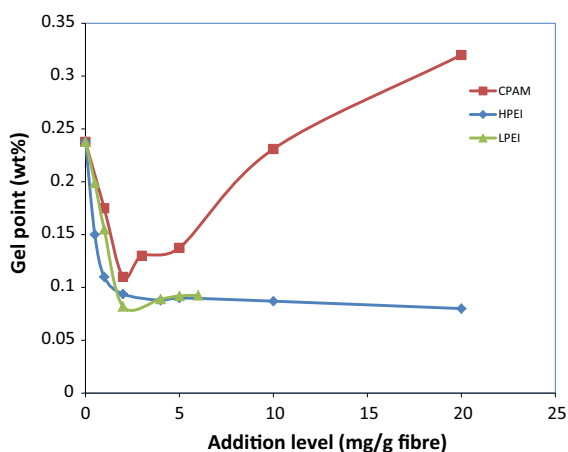
Fig. 3 Gel point as a function of polyelectrolyte type and concentration

1 mg/g polymer was added, whereas it declined to 0.16 wt% for LPEI and 0.09 wt% for HPEI. Interestingly, the minimum gel point was achieved at 2 mg/g for both CPAM and LPEI. Gel point kept increasing as the addition level increased from 2 to 10 mg/g for CPAM, where the gel point was almost same as the blank MFC. Above CPAM addition of 10 mg/g, the gel point kept increasing. However, both HPEI and LPEI were observed to have a stable gel point after reaching its minimum gel point. The difference observed between the gel point trends obtained with CPAM and PEI shows that there are likely to be different mechanisms by which the two types of polymer interact with cellulose nanofibres. CPAM is a linear polymer with high flexibility and is able to adsorb forming loops and tails on MFC, resulting in steric repulsion at high dosages. The gel point curve of CPAM where it reduces to reach a minimum and then increases steadily is typical of a polyelectrolyte stabilisation by bridging where the minimum corresponds to roughly half surface coverage (Raj et al. 2015). PEI is a branched dendrimer and may not cause steric repulsion resulting in the gel point remaining low even at high dosages.

Figure 4 shows the relationship between the maximum dewatering force of the cellulose nanofibre suspension and the addition dosage of two polymers, HPEI and CPAM. It should be noted that that initial MFC solids concentration of 0.15 wt% is below the gel point for low levels of polymer addition as well as

Fig. 4 Dewatering force as a function of polymer concentration for CPAM and HPEI. *Error bars* represent 95 % confidence interval. MFC concentration = 0.15 wt%
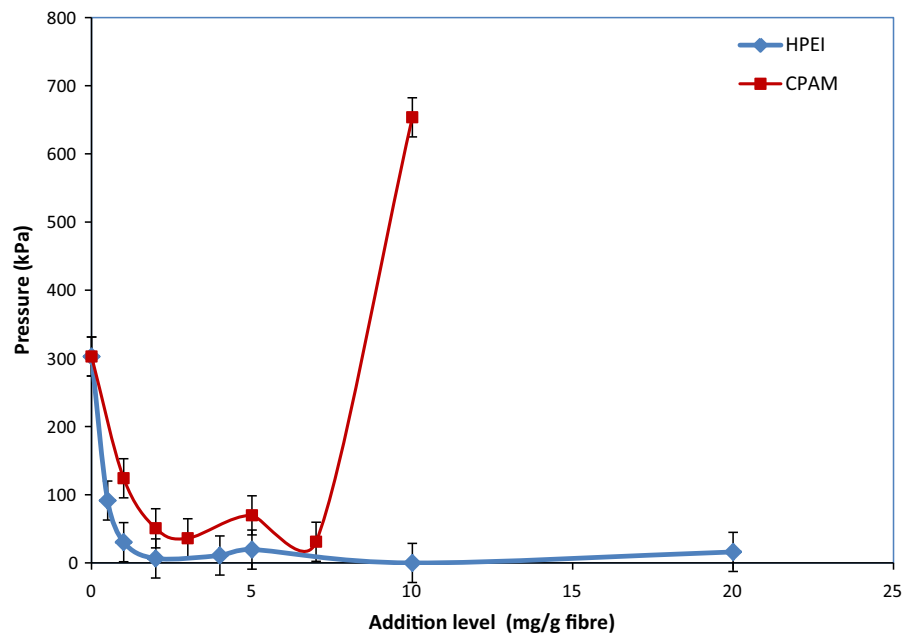

high levels of CPAM addition and is above the gel point for intermediate levels of polymer addition. However, there is no indication in the data in Fig. 4 of any transition when passing through the gel point. This suggests that even when the initial solids concentration is somewhat below the gel point, initial dewatering rapidly creates a filter mat from the partly flocculated suspension. This was confirmed with measurements at 0.3 % solids content, which are not reported here, which showed the same trend with polymer addition over the range 0–10 mg/g of CPAM addition.

PEI and CPAM show two different modes of drainage as a function of concentration, when added to a nanocellulose suspension. For addition with either CPAM or HPEI, the dewatering force was significantly reduced with lower addition levels. HPEI showed a larger decrease of dewatering force at all addition levels of polymer. At some high addition levels of HPEI, the maximum dewatering pressure of the MFC suspension even approached 0 kPa. Dewatering force decreased with addition of CPAM up to the addition levels of 7 mg/g and then increased. At high addition levels of CPAM, the maximum dewatering pressure was very high, whereas with HPEI addition the dewatering force remained low and stable even at very high addition levels up to 20 mg/g.

It can be observed that the trend of dewatering force is similar to the gel point trend (Fig. 3) with a small increase for both measurements at 5 mg/g. While dewatering force drops to a minimum at higher addition levels of HPEI, it suddenly increased with the addition of 10 mg of CPAM/g of MFC.

Figure 5 shows the time required to dewater the nanofibre suspension when forming the membrane layer onto the hardwood sheet support. The initial nanofibre layer solids content was below the gel point solids concentration for all levels of polyelectrolyte addition. The behaviour with polymer addition can be divided into two categories. For CPAM addition, the dewatering time decreased as more CPAM was added, until it reached a minimum point, and started to increase between addition level 2 and 3 mg/g. For PEI addition, the suspension dewatering time trend was similar to the trends observed in gel point and dewatering pressure where the dewatering time for both HPEI and LPEI decreased and then stayed the same with increasing addition levels. The dewatering time of the suspension with HPEI was always lower than that with LPEI. All CPAM dewatering time data fell below the LPEI data except at the crossover point which occurred at 5 mg/g polymer addition. There was also a crossover between HPEI and CPAM which occurred at 3 mg/g.

Fig. 5 Dewatering time in sheet forming as a function of the type and polyelectrolyte addition level
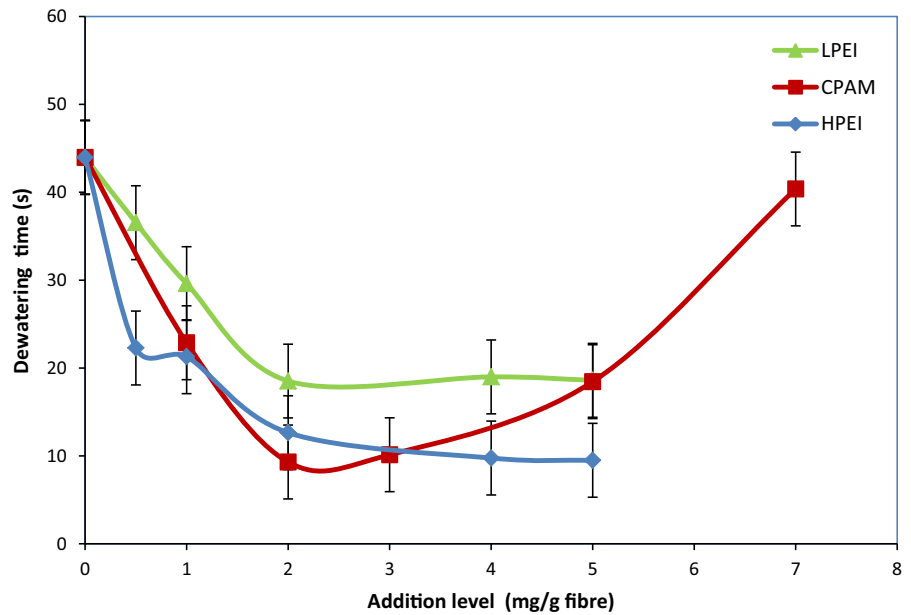
Sheet property measurements

Air permeance is an indication of membrane structure and is controlled by both the pore volume, diameter and pore network connectivity (Ek et al. 2009). Figure 6 shows the relation between the air permeability of MFC-paper composite membrane as a function of addition levels of polymers. Both LPEI and HPEI show a similar trend, with an increase from 0.058 μm/Pa s to a maximum of 0.072 and 0.099 μm/Pa s for LPEI and HPEI at addition level of 2 mg/g. HPEI is more effective at increasing the air permeability, with air permeability rising by 46 % at the maximum compared to only 25 % for LPEI addition. CPAM has a similar

Fig. 6 Air permeability of air dried MFC-paper composite sheet as a function of the polyelectrolyte type and concentration
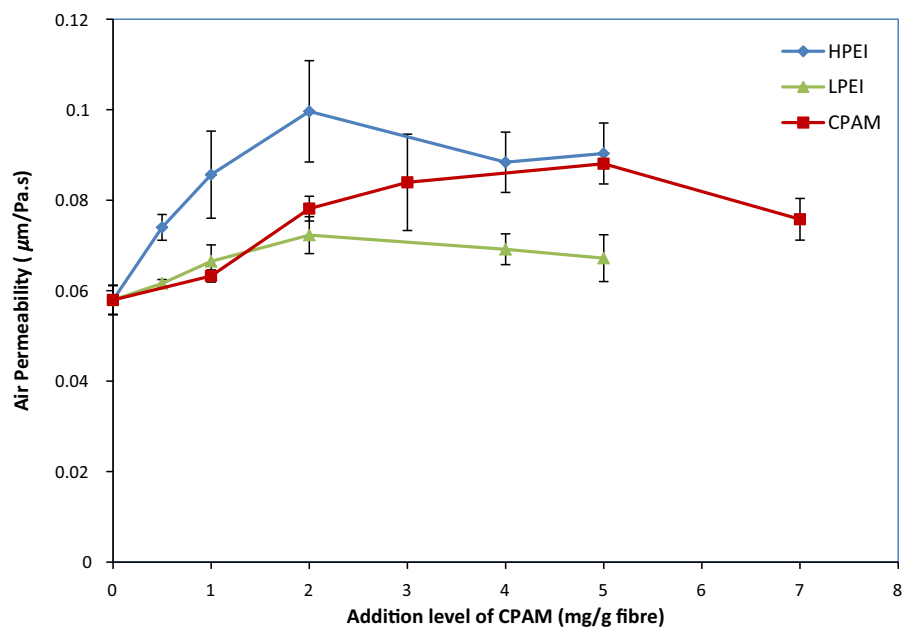
effect to HPEI when adding 5 mg CPAM/g of fibre. Among the three polymers, HPEI can achieve the highest permeability with the least dosage. However, LPEI has a weak effect on air permeance. Another interesting point is that maximum air permeance is observed at addition level of 2 mg of polymer/g of MFC for both LPEI and HPEI, which is similar to what was observed in the dewatering time results.

Although a reduction in gel point creates more porous sheets, previous work has shown that with polymer addition, the tensile index of MFC–CPAM sheets did not significantly change over the limited reduction of density achievable with polymer addition (Varanasi and Batchelor 2014). The tensile strength increased slightly from 71 kNm/kg (no CPAM addition) to 82 kNm/kg (2 mg/g CPAM addition).

Figure 7 shows the relation between the pressure at which water passes through the MFC membrane, at the indicated water flux, at different addition levels of CPAM and PEI. For CPAM, two different fluxes (72.9 and 36.5 LMH) were measured. Both show a trend that corresponds to the gel point line, with its decrease at low addition levels until 2 mg/g and increase at high addition levels. The pressure of flux at 72.9 LMH is approximately double the pressure at 36.5 LMH. As with CPAM, LPEI trend line is also similar to its counterpart in the gel point graph, with all values below the CPAM trend line. Thus, adding LPEI during sheet forming reduces the pressure
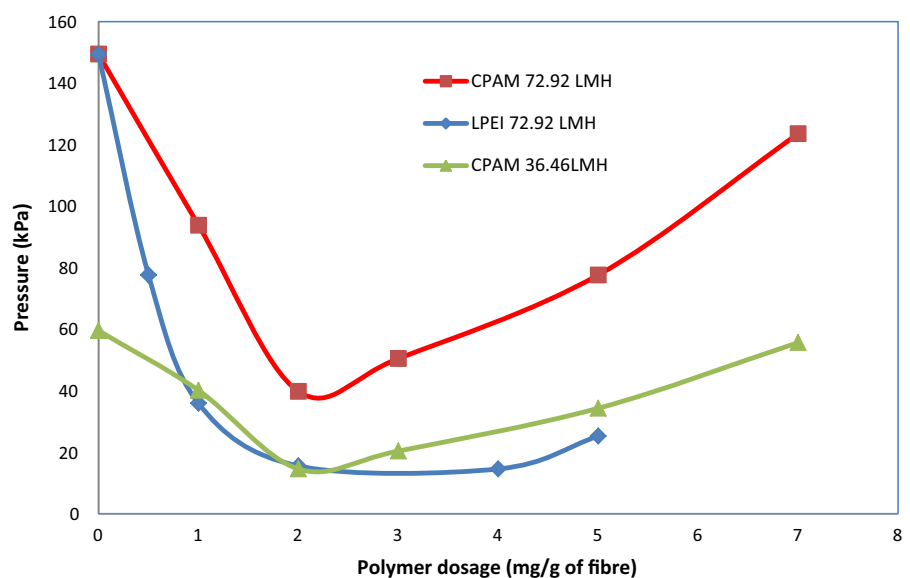
required to achieve a given flux through the membrane. This finding for nanocellulose membranes is very similar to the behaviour of CPAM on regular bagasse pulp fibre sheets (Rainey et al. 2010a, b).

Discussion

As the results have shown, both sheet forming properties and sheet properties such as air permeance are changed with polymer addition, with the change in gel point and that the change in property often seemed to correlate at least approximately with the development of the gel point curves with the addition of the different polymers. It is interesting to see the correlation between suspension or sheet properties and the gel point. To allow the correlation to be shown on the same graph, all the properties data are normalized by having been converted into a fraction using the property value measured for the MFC sheet alone without polymer addition as the reference point equal to 1.0. This point is shown as the large circular point on the graph.

Figure 8 shows the fractional change in property for suspension dewatering pressure, suspension dewatering time, membrane pressure at a flux of 72.92 and 36.46 LMH, and membrane air permeance as a function of gel point.

Fig. 7 Pressure as a function of polymer addition level at fixed flux

(a)

$y = 4.0491x - 0.3212$
$R^2 = 0.8922$

■ CPAM ◆ HPEI

(a)

● Dewatering pressure   ■ Dewatering time

■ Dewatering time   ◆ Air permeance

✕ Pressure at a flux of 36.46 LMH   ● Pressure at a flux of 72.92 LMH
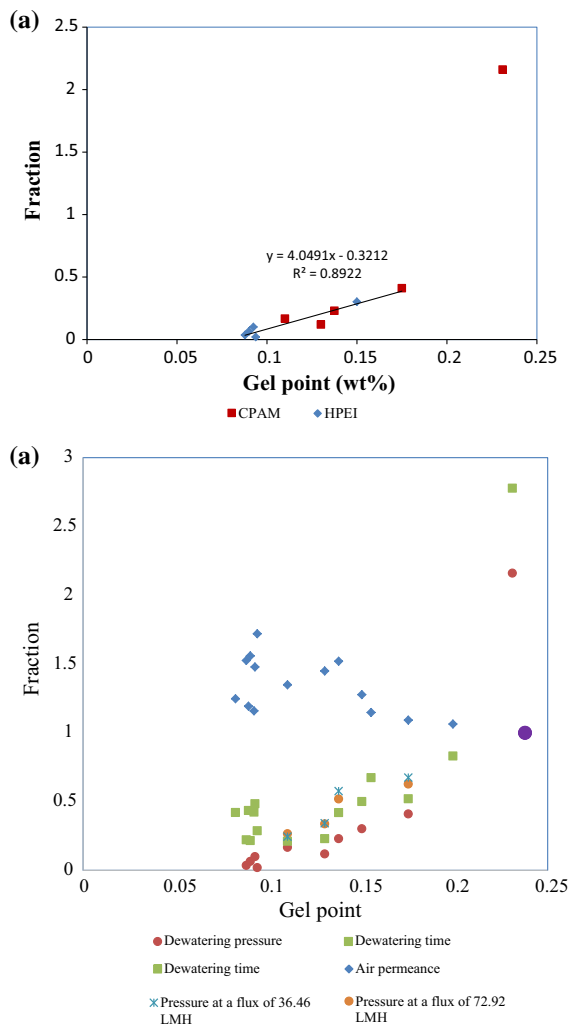
Fig. 8 Fractional property change of **a** Dewatering pressure **b** all properties as a function of gel point. The *large circular point* is the reference point

There is a strong relationship between gel point and the fractional change of all properties. This master curve suggest that the independent variable controlling the behaviour of the nanocellulose suspension and the resulting composites is indeed the structure of the flocculated nanocellulose network, best expressed in terms of gel point. No distinction is observed between the type and morphology of polyelectrolyte used. This can be shown from Fig. 8a where all the data points for dewatering pressure fall close to the straight line with no distinction between each polymer type. There was an exception of one data point that occurred at a very high dosage of CPAM which may have been due to a

change in the viscosity of the suspension. Table 1 shows the fitting statistics for all the properties. It can be seen that dewatering pressure and pressure at a fix flux data fitted the respective straight lines well.

For dewatering pressure, dewatering time, pressure of a fixed flux, the values decreased with decrease in gel point with almost all of the values falling under 1.0. Only when an excess amount of CPAM of 10 mg/g were added, did suspension dewatering pressure and dewatering time have higher values than the reference point.

Dewatering pressure, dewatering time and membrane permeability all have similar trends and the fractional decrease in all of the three is at least 50 %, at the lowest gel point. On the other hand, the air permeability increased with decreasing gel point, consistent with the decreased pressure required for a fixed flux of water through the membrane.

Conclusion

Polyelectrolyte addition to a nanocellulose suspension is efficient at improving processability and nanocellulose film properties. In this study, three polyelectrolytes were investigated: a high molecular weight linear CPAM, a high and a low molecular weight PEI (HPEI and LPEI). The addition of either PEI or CPAM to MFC reduced the gel point significantly until an addition level of 2 mg/g, after which, further addition of CPAM increased the gel point while further addition of PEI did not change the gel point. The minimum gel point achieved 0.08 kg/m^3, compared to 0.24 kg/m^3 without polymer addition.

We showed that the gel point was linearly correlated both with suspension dewatering characteristics and with the filtration properties of the formed sheet. A decrease in gel point reduced the pressure required to dewater the suspension at a given rate as well as the total time required to form a sheet. The more open suspension structure, with lower gel point, was also partially preserved in the sheets made from the suspension, which showed higher air permeability and lower pressure to achieve a given liquid flux through the suspension.

The major controlling factor was gel point, independent of the type of polymer used, despite the expected different mode of action of PEI compared to CPAM.

Table 1 Fitting statistics for each property

Property	Equation of straight line	R^2
Dewatering pressure	y = 4.0491x − 0.3212	0.8922
Dewatering time	y = 4.0419x − 0.0595	0.6868
Air permeance	y = −2.8903x + 1.6887	0.409
Pressure at a flux of 36.46 LMH	y = 5.7008x − 0.3337	0.9348
Pressure at a flux of 72.92 LMH	y = 5.65x − 0.3431	0.9682

The existence of a master curve for each property with gel point, highlights the strong potential to engineer cellulose nanofibre suspension and sheet properties using polyelectrolyte addition.

References

Ek M, Gellerstedt G, Henriksson G (2009) Paper products physics and technology. Walter de Gruyter, Berlin

Fukuzumi H, Saito T, Iwata T, Kumamoto Y, Isogai A (2008) Transparent and high gas barrier films of cellulose nanofibers prepared by TEMPO-mediated oxidation. Biomacromolecules 10(1):162–165. doi:10.1021/bm801065u

Hubbe MA, Venditti RA, Rojas OJ (2007) Review of factors affecting the release of water from cellulosic fibers during paper manufacturer. BioResources 2(3):500–533

Landman KA, White LR, Buscall R (1988) The continuous-flow gravity thickener: steady state behavior. AIChE J 34(2):239–252. doi:10.1002/aic.690340208

Lowys M-P, Desbrieres J, Rinaudo M (2000) Rheological characterization of cellulosic microfibril suspensions. Role of polymeric additives. Food Hydrocoll 15:25–32

Lu J, Askeland P, Drzal LT (2008) Surface modification of microfibrillated cellulose for epoxy composite applications. Polymer 49(5):1285–1296. doi:10.1016/j.polymer.2008.01.028

Martinez DM, Buckley K, Jivan S, Lindstrom A, Thiruvengadaswamy R, Olson JA, Ruth TJ, Kerekes RJ (2001) Characterizing the mobility of papermaking fibres during sedimentation. In: 12th fundamental research symposium. The science of papermaking, pp 225–254

Mosse WKJ, Boger DV, Simon GP, Garnier G (2012) Effect of cationic polyacrylamides on the interactions between cellulose fibers. Langmuir 28(7):3641–3649. doi:10.1021/la2049579

Nakagaito AN, Yano H (2005) Novel high-strength biocomposites based on microfibrillated cellulose having nano-order-unit web-like network structure. Appl Phys A 80(1):155–159. doi:10.1007/s00339-003-2225-2

Nanko H, Pan S (2003) Visualization of polymer adsorption on pulp fiber: polyacrylamide. In: Proceedings of 2003 TAPPI spring technical conference, Chicago, IL

Nasser MS, James AE (2006) The effect of polyacrylamide charge density and molecular weight on the flocculation and sedimentation behaviour of kaolinite suspensions. Sep Purif Technol 52(2):241–252. doi:10.1016/j.seppur.2006.04.005

Nasser MS, James AE (2007) Effect of polyacrylamide polymers on floc size and rheological behaviour of kaolinite suspensions. Colloids Surf, A 301(1–3):311–322. doi:10.1016/j.colsurfa.2006.12.080

Rainey TJ, Doherty WOS, Martinez DM, Brown RJ, Dickson A (2010a) The effect of flocculants on the filtration of bagasse pulp pads. Tappi J, pp 7–14

Rainey TJ, Moghaddam L, Doherty WOS (2010b) The effect of flocculants, shear, vacuum and depithing on the formation of thin bagasse pulp pads. Nord Pulp Pap Res J 25(4):434–440. doi:10.3183/NPPRJ-2010-25-04-p434-440

Rainey T, Doherty WS, Martinez DM, Brown R, Kelson N (2011) Pressure filtration of Australian bagasse pulp. Transp Porous Med 86(3):737–751. doi:10.1007/s11242-010-9649-x

Raj P, Varanasi S, Batchelor W, Garnier G (2015) Effect of cationic polyacrylamide on the processing and properties of nanocellulose films. J Colloid Interface Sci 447:113–119. doi:10.1016/j.jcis.2015.01.019

Sakurada I, Nukushina Y, Ito T (1962) Experimental determination of the elastic modulus of crystalline regions in oriented polymers. J Polym Sci 57(165):651–660. doi:10.1002/pol.1962.1205716551

Sehaqui H, Liu A, Zhou Q, Berglund LA (2010) Fast preparation procedure for large, flat cellulose and cellulose/inorganic nanopaper structures. Biomacromolecules 11(9):2195–2198. doi:10.1021/bm100490s

Siró I, Plackett D (2010) Microfibrillated cellulose and new nanocomposite materials: a review. Cellulose 17(3):459–494. doi:10.1007/s10570-010-9405-y

Syverud K, Stenius P (2009) Strength and barrier properties of MFC films. Cellulose 16(1):75–85. doi:10.1007/s10570-008-9244-2

Turbak AF, Snyder FW, Sandberg KR (1983) Microfibrillated cellulose, a new cellulose product: properties, uses, and

commercial potential. J Appl Polym Sci: Appl Polym Symp 37:815–827

Varanasi S, Batchelor W (2014) Superior non-woven sheet forming characteristics of low-density cationic polymer–cellulose nanofibre colloids. Cellulose 21(5):3541–3550. doi:10.1007/s10570-014-0370-8

Varanasi S, He R, Batchelor W (2013) Estimation of cellulose nanofibre aspect ratio from measurements of fibre suspension gel point. Cellulose 20(4):1885–1896. doi:10.1007/s10570-013-9972-9

Vesterinen A, Seppala J (2008) Rheological study of microfibrillar cellulose and dynamic mechanical analysis of paper sheet. Annu Trans Nord Rheol Soc 16:259–262

Zhang L, Batchelor W, Varanasi S, Tsuzuki T, Wang X (2012) Effect of cellulose nanofiber dimensions on sheet forming through filtration. Cellulose 19(2):561–574. doi:10.1007/s10570-011-9641-9

Zhu H, Fang Z, Preston C, Li Y, Hu L (2014) Transparent paper: fabrications, properties, and device applications. Energy Environ Sci. doi:10.1039/C3EE43024C